Am J Physiol Gastrointest Liver Physiol 304: G655–G661, 2013.
First published January 31, 2013; doi:10.1152/ajpgi.00472.2012.

Endocytic pathway of exogenous iron-loaded ferritin in intestinal epithelial (Caco-2) cells

Elmer Antileo,[1] Carolina Garri,[1] Victoria Tapia,[1] Juan Pablo Muñoz,[2] Mario Chiong,[3] Francisco Nualart,[4] Sergio Lavandero,[3,5] Juan Fernández,[1] and Marco T. Núñez[1,6]

[1]*Facultad de Ciencias, Departamento de Biología, Universidad de Chile, Santiago, Chile;* [2]*Department of Biochemistry and Molecular Biology, Institute for Research in Biomedicine (IRB Barcelona), Universitat de Barcelona and CIBERDEM, Barcelona, Spain;* [3]*Facultad Ciencias Químicas y Farmacéuticas & Facultad de Medicina, Centro de Estudios Moleculares de la Célula, Universidad de Chile, Santiago, Chile;* [4]*Departament of Cell Biology and Center for Advanced Microscopy CMA BIO-BIO, Universidad de Concepción, Concepción, Chile;* [5]*Department of Internal Medicine (Cardiology Division), University of Texas Southwestern Medical Center, Dallas, Texas; and* [6]*Millennium Institute of Cell Dynamics and Biotechnology, Santiago, Chile*

Submitted 12 December 2012; accepted in final form 26 January 2013

Antileo E, Garri C, Tapia V, Muñoz JP, Chiong M, Nualart F, Lavandero S, Fernández J, Núñez MT. Endocytic pathway of exogenous iron-loaded ferritin in intestinal epithelial (Caco-2) cells. *Am J Physiol Gastrointest Liver Physiol* 304: G655–G661, 2013. First published January 31, 2013; doi:10.1152/ajpgi.00472.2012.—Ferritin, a food constituent of animal and vegetal origin, is a source of dietary iron. Its hollow central cavity has the capacity to store up to 4,500 atoms of iron, so its potential as an iron donor is advantageous to heme iron, present in animal meats and inorganic iron of mineral or vegetal origin. In intestinal cells, ferritin internalization by endocytosis results in the release of its iron into the cytosolic labile iron pool. The aim of this study was to characterize the endocytic pathway of exogenous ferritin absorbed from the apical membrane of intestinal epithelium Caco-2 cells, using both transmission electron microscopy and fluorescence confocal microscopy. Confocal microscopy revealed that endocytosis of exogenous AlexaFluor 488-labeled ferritin was initiated by its engulfment by clathrin-coated pits and internalization into early endosomes, as determined by codistribution with clathrin and early endosome antigen 1 (EEA1). AlexaFluor 488-labeled ferritin also codistributed with the autophagosome marker microtubule-associated protein 1 light chain 3 (LC3) and the lysosome marker lysosomal-associated membrane protein 2 (LAMP2). Transmission electron microscopy revealed that exogenously added ferritin was captured in plasmalemmal pits, double-membrane compartments, and multivesicular bodies considered as autophagosomes and lysosomes. Biochemical experiments revealed that the lysosome inhibitor chloroquine and the autophagosome inhibitor 3-methyladenine (3-MA) inhibited degradation of exogenously added ^{131}I-labeled ferritin. This evidence is consistent with a model in which exogenous ferritin is internalized from the apical membrane through clathrin-coated pits, and then follows a degradation pathway consisting of the passage through early endosomes, autophagosomes, and autolysosomes.

intestinal iron absorption; ferritin; endocytosis

THE MAINTENANCE OF SYSTEMIC iron homeostasis is vital to human health, given that iron deficiency is the most common nutrition-related pathology worldwide. Iron's essentiality, coupled to its scarcity in aqueous oxidative environments, has compelled live organisms to develop mechanisms that ensure an adequate iron supply, with disregard to the long-term deleterious effects derived from iron accumulation (14, 36). Currently there are two fully characterized sources of dietary iron, namely heme iron present in hemoglobin and myoglobin and nonheme iron or inorganic iron present in vegetables. The divalent metal transporter 1 mediates the uptake of inorganic iron while the uptake of heme iron is most probably carried out by heme carrier protein 1 (HCP1), which mediates luminal heme uptake in a temperature- and concentration-dependent manner (46). Recent evidence has shown that HCP1 is also a proton-coupled folate transporter (PCFT), since a homozygous mutation in its gene results in hereditary folate malabsorption (40). In addition, a study on the transport characteristics of PCFT/HCP1 showed that heme and folate compete for transport in everted duodenum from hypoxic but not from normal mice (22). Overall, the data support a dual function for PCFT/HCP1, primarily as a folate transporter but with a lower affinity for heme.

A third source of dietary iron is currently emerging: ferritin, a multisubunit protein containing caged iron (26, 52, 53). Indeed, a recent study demonstrated that ferritin iron is absorbed from the intestinal lumen by a process different from heme and inorganic iron absorption, and, once it is absorbed, it behaves as a slow-release iron donor (54). Vertebrate and plant ferritins consist of 24 α-helical subunits of H- and L-ferritin that assemble to form a hollow shell with an outer diameter of 12 nm and an inner diameter of 8 nm (12). Vertebrate ferritins catalyze the oxidation of ferrous ion, promoting the formation of a ferric oxyhydroxide mineral within their inner cavity (23). The average number of iron atoms per ferritin varies from zero to up to 4,000, averaging 1,000–1,500 (30, 52). Specific ferritin binding has been identified in a number of cells and tissues, including liver, placenta, and hepatoma and lymphoid, erythroid, and endothelium cells (1, 7, 35, 41, 48). In some cell types, binding of ferritin is followed by internalization. Erythroid cells take up ferritin, and the transferred iron is sufficient to influence iron-dependent gene expression (39).

There seems to be more than one receptor that mediates ferritin binding. The T cell immunoglobulin and mucin domain-2 (TIM-2) receptor binds H-ferritin, allowing for its entry into endosomes (5, 11). TIM-2 expression is restricted to mouse B lymphocytes, embryonic liver, and kidney mouse cells, and to rat oligodendrocytes (5, 55). Recently, the scavenger receptor class A, member 5 (Scara5) was identified in developing mouse kidney cells as an L-ferritin receptor on the

Address for reprint requests and other correspondence: M. T. Núñez, Departamento de Biología, Facultad de Ciencias, Universidad de Chile, Las Palmeras 3425, Santiago, Chile (e-mail: mnunez@uchile.cl).

basis that its presence on the surface of MSC-1 cells increases absorption of ferritin iron (24). Scara5 levels respond to cell iron status, since iron deficiency increases sevenfold its expression in cells lacking transferrin receptors, which are responsible for primary iron uptake. A third ferritin receptor is human transferrin receptor 1 (hTfR1) that binds both H-ferritin and transferrin (25). H-ferritin binds to hTfR1 in six human cell lines that include T cell and B cell precursors, ovarian cancer cells, and kidney transformed cells (25). Submicromolar concentrations of transferrin inhibit binding of H-ferritin to hTfR1, so in the presence of blood plasma the efficiency of TfR1-mediated H-ferritin endocytosis should be low.

Previous work demonstrated that exogenous soybean ferritin is internalized and degraded by an adaptor protein-2 (AP-2)-dependent process, since knockdown of the μ_2-subunit effectively decreases its internalization and degradation (45). In a similar study, ferritin was shown to undergo internalization by a G protein-dependent endocytic process (18). The involvement of AP-2 in horse spleen ferritin (hsFn) internalization and degradation suggests that exogenous ferritin is internalized and degraded through the classic route of clathrin-mediated endocytosis.

At the cellular level, the route by which ferritin is degraded and iron becomes available for intestinal absorption is unknown. In the present study, we characterized the degradation route of exogenous ferritin, using Caco-2 cells as a cellular model of intestinal epithelium. Our results indicate that, after internalization from clathrin-coated pits, exogenous ferritin is present in early endosomes, autophagosomes, and lysosomes. Inhibitors of lysosomes or autophagosomes significantly inhibited ferritin degradation. The characterization of the ferritin endocytosis process paves the way for further studies intended to intervene this iron acquisition route.

MATERIALS AND METHODS

Ferritin. Commercial hsFn (F-4503; Sigma) was diluted in PBS pH 7.4, centrifuged to 10,000 *g* for 30 min, and then filtered through a Sephacryl S400 column equilibrated in PBS. The main protein peak was collected, and the iron content of ferritin was estimated by its absorbance at 420 nm (28). The iron content of the hsFn used in this study contained an average of 3,200 iron atoms/ferritin molecule, as determined by atomic absorption spectroscopy.

For confocal microscopy, hsFn was labeled with the fluorescent probe Alexa Fluor 488 using the Alexa Fluor Protein Labeling Kit (Invitrogen-Molecular Probes). The labeled protein (hsFn-AlexaFluor 488) was stored in the dark at 4°C. For studies of protein degradation, ferritin was labeled with ^{131}I (Chilean Commission of Nuclear Energy) using the Iodogen reagent (Pierce Chemical) as described (45).

Antibodies. The following antibodies were used in this study: anti-clathrin heavy chain mouse monoclonal antibody (Calbiochem); anti-early endosome antigen (EEA1) mouse monoclonal antibody (BD Transduction Laboratories); anti-autophagy-related protein light chain 3 (LC3) rabbit polyclonal antibody (Santa Cruz Biotechnology)

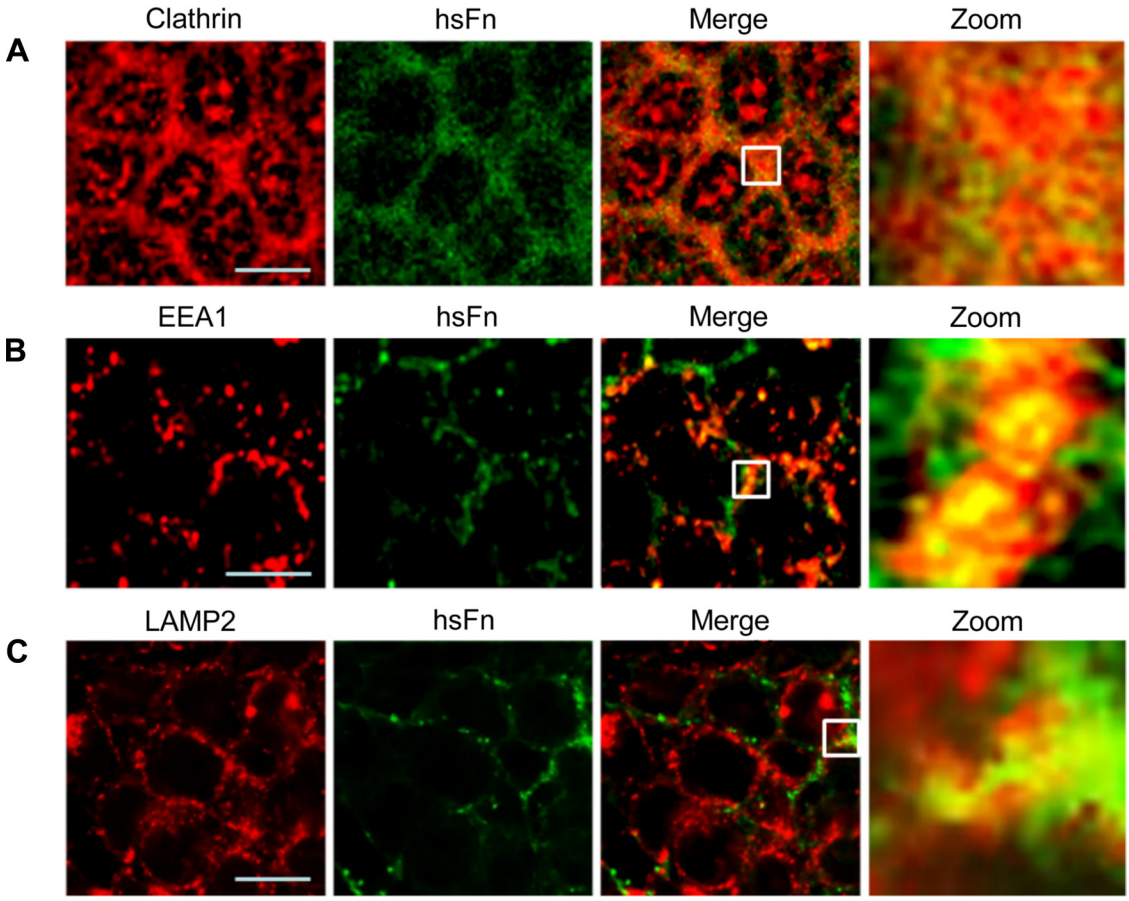

Fig. 1. Codistribution of exogenous horse spleen ferritin (hsFn) with endosomal markers. Caco-2 cells grown in bicameral inserts were incubated for 20 min at 37°C with 20 nM hsFn-AlexaFluor 488. Cells were then fixed and immunostained for the endosomal markers clathrin (*A*) and early endosome antigen 1 (EEA1, *B*) or for the lysosomal marker lysosomal-associated membrane protein 2 (LAMP2, *C*) as described in MATERIALS AND METHODS. Scale bars are 20 μm.

and anti-lysosomal-associated membrane protein 2 (LAMP2) mouse monoclonal antibody (BD Biosciences). Secondary antibodies were AlexaFluor 546-labeled anti-rabbit- or anti-mouse-IgG (Invitrogen-Molecular Probes).

Cells. Human Caco-2 cells (ATCC HTB37) grown in DMEM supplemented with 10% fetal bovine serum was used. For confocal microscopy, cells were grown on glass cover slips for 12–14 days before the experiment. Under these conditions, the cells grow as a polarized monolayer with the apical/microvillus membrane toward the culture medium. For transmission electron microscopy studies, cells were grown for 14–16 days in bicameral inserts as described (51).

Confocal and transmission electron microscopy. Cells were incubated for 45 min at 37°C with 20 nM hsFn-AlexaFluor 488 (Invitrogen-Molecular Probes). After being washed, the cells were fixed with freshly prepared 4% paraformaldehyde and immunostained for either clathrin, EEA1, LAMP2, or LC3 (Invitrogen-Molecular Probes) as previously described (45). In all cases, the secondary antibody was labeled with AlexaFluor 546. Samples were mounted in Gel Mount (Sigma Chemical) and observed with a Zeiss LSM 510 Meta confocal microscope (Carl Zeiss, Jena, Germany).

For transmission electron microscopy, cells were incubated for 45 min at 37°C with 20 nM hsFn and then fixed with 50% Karnovsky fixative (19). Samples were then dehydrated in graded ethanol and embedded under vacuum in Epon 812 as described (6). Epon blocks were cut to 70-nm slices and were then sequentially stained with 0.04% bismuth subnitrate, saturated uranyl citrate, and 0.25% lead citrate. The latter staining procedure enhances ferritin detection (2). Sections were examined with a FEI CM-12 transmission electron microscope.

Inhibition of lysosomal and autophagosomal activity. Ferritin proteolysis was determined by measuring the rate of degradation of ^{131}I-labeled hsFn as described (45). Cells were preincubated for 30 min at 37°C either with 100 μM chloroquine [a lysosomal inhibitor (57)] or 10 mM 3-methyladenine [3-MA, an autophagy inhibitor (49)] followed by incubation for 30 min with 20 nM ^{131}I-hsFn.

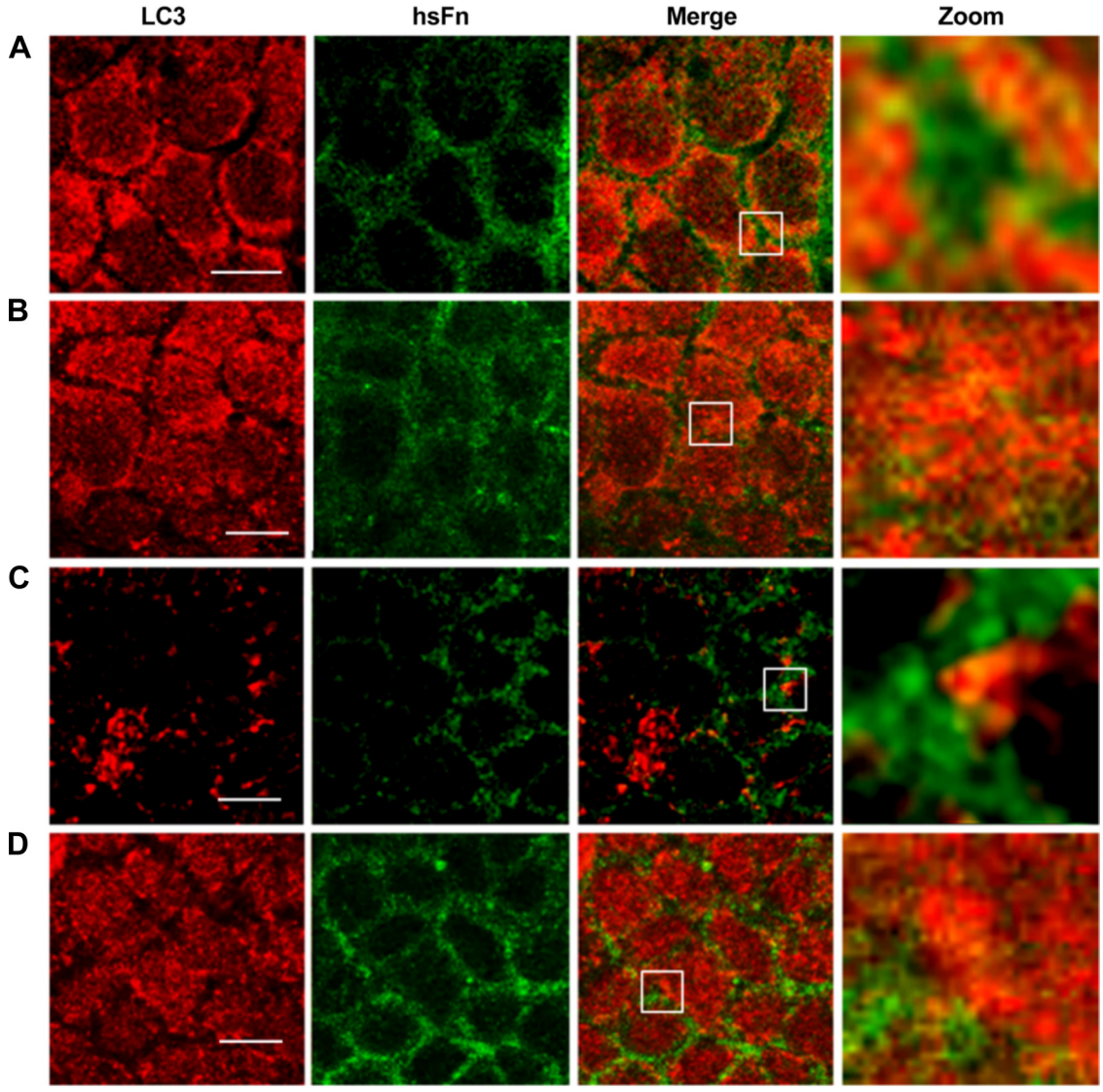

Fig. 2. Codistribution of internalized hsFn with autophagosomal compartments. *A*: control cells were incubated for 20 min with 20 nM hsFn-AlexaFluor 488, fixed, and immunostained for the autophagosomal marker light chain 3 (LC3) and developed with AlexaFluor 546-labeled secondary antibody. *B*: cells were incubated overnight in the absence of serum (serum deprivation) before incubation with hsFn labeled with AlexaFluor 488 and immunostaining for LC3. Inhibition of autophagosomal or lysosomal activity was achieved by preincubation for 30 min at 37°C with either 10 mM 3-methyladenine (3-MA, *C*) or 100 μM chloroquine (*D*). Scale bars are 20 μm.

RESULTS

Exogenous hsFn codistributes with markers of the degradation route of clathrin-mediated endocytosis. Previous work demonstrated that exogenous soybean ferritin is internalized and degraded by an AP-2-dependent process, since the knockdown of the μ_2-subunit effectively decreases its internalization and degradation (45). The involvement of AP-2 in hsFn internalization and degradation suggests that exogenous ferritin is internalized and degraded through the classic route of clathrin-mediated endocytosis, which includes internalization through coated pits, residence in sorting endosomes, and maturation through multivesicular bodies into late endosomes and lysosomes (43). Based on the hypothesis that exogenous ferritin follows this degradation route, we characterized cellular endosomal compartments that codistribute with endocytosed ferritin. To this end, hsFn was labeled with the fluorescent probe Alexa 488 to determine by immunofluorescence its codistribution with clathrin, the early endosome marker EEA1, and the late endosome/lysosome marker LAMP2.

Codistribution of hsFn with clathrin was clearly observed in apical areas of Caco-2 cells (Fig. 1*A*), indicating that both molecules share the same subcellular distribution. Similarly, codistribution of hsFn with the early endosome marker EEA1 (Fig. 1*B*) and the late endosome-lysosome marker LAMP2 (Fig. 1*C*) was observed. Fluorescence of both EEA1 and hsFn-Alexa 488 was detected in the peripheral cytoplasm near the cell membrane. Regions where both EEA1 and hsFn-Alexa 488 fluorescence signals coexist were readily noticeable (Fig. 1*B*). LAMP2 was distributed throughout the cytoplasm, although the fluorescence was more pronounced in the peripheral cytoplasm. The codistribution of hsFn and LAMP2 signals was discrete, circumscribed to small granular regions in the peripheral cytoplasm (Fig. 1*C*).

Internalized ferritin reaches autophagic compartments. The autophagosome-lysosome pathway contributes to the degradation of senescent organelles and proteins, including endogenous ferritin (13, 32). Because a connection between the phagocytic and autophagic systems has been acknowledged (8), we hypothesized that the degradation routes for endogenous and exogenous ferritin may coincide at the autophagosome level. To test this hypothesis, we carried out confocal microscopy experiments to search for possible interactions between hsFn and LC3, a component of the autophagosome membrane that has been widely used to study autophagy (33, 50).

Codistribution of hsFn-Alexa 488 with LC3 was evaluated under normal experimental conditions and under serum deprivation, a condition that triggers autophagy (34). Under control culture conditions (10% FCS medium), there was a significant coincidence between hsFn and LC3 fluorescence in cytoplasmic domains (Fig. 2*A*), suggesting that both molecules share the same subcellular localization. Induction of autophagy by serum deprivation resulted in enhanced LC3 fluorescence and multiple spots of codistribution with hsFn throughout the cytoplasm (Fig. 2*B*). To further assess the interaction between hsFn and autophagosomes, codistribution of hsFn and LC3 was studied after treatment with 3-MA, a specific autophagy inhibitor that suppresses the formation of autophagosomes through the inhibition of class III phosphoinositide 3-kinase (4, 38). Inhibition of autophagosome formation by 3-MA resulted in a decrease of LC3 fluorescence intensity (Fig. 2*C*). This decrease was possibly the consequence of inhibition of the expression of LC3 by 3-MA. The intracellular hsFn fluorescence signal also decreased and HsFn-LC3 codistribution was greatly impaired (Fig. 2*C*). Similarly, inhibition of lysosome activity with chloroquine resulted in a decrease in LC3 fluorescence intensity and a decrease in the hsFn fluorescence signal compared with the control (Fig. 2*D*).

Intracellular distribution of internalized ferritin. Transmission electron microscopy in Caco-2 cells preincubated with iron-loaded hsFn showed electron-dense particles 6–7 nm in diameter (Fig. 3*A*). This particle size corresponds to that of ferritin molecules with high iron content (12). Incubation of cells with hsFn resulted in the presence of electrodense aggregates inside the cells (Fig. 3*B*) that were absent in cells not incubated with hsFn (Fig. 3*C*). Analysis of bicameral insert-grown cells revealed that they form a monolayer of polarized cells whose apical surface formed typical microvilli (Fig. 4*A*). After incubation, hsFn was detected in several apical compartments, including deep plasmalemmal membrane pits (Fig. 4*B*) and tubule-vesicular structures, located in the peripheral cytoplasm (Fig. 4, *C* and *D*) described before as early endosomes (20). Besides, hsFn was detected in ~500-nm double-membrane structures with the morphological features of autopha-

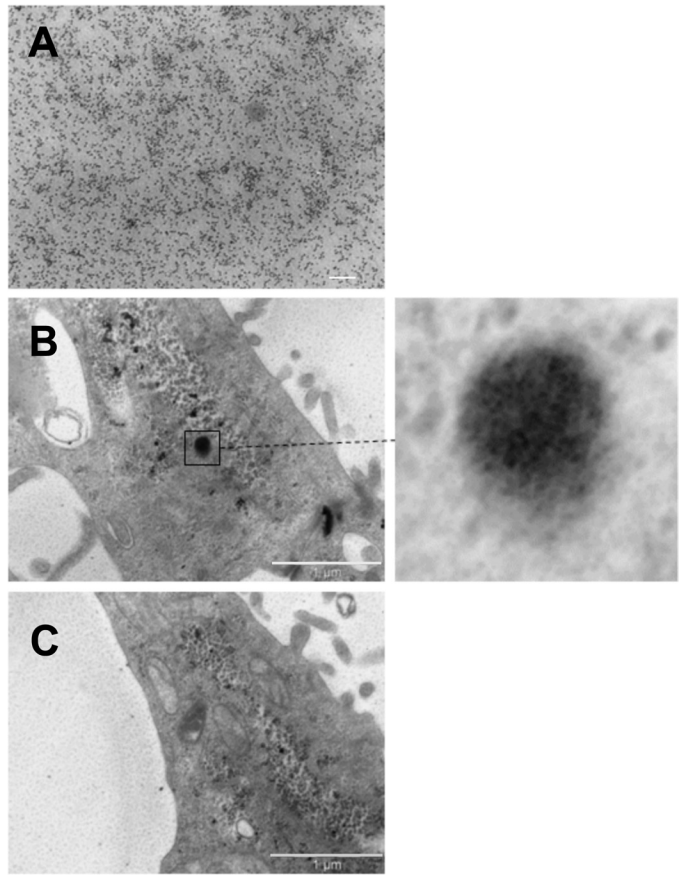

Fig. 3. Micrograph from transmission electron microscopy illustrating hsFn detection. *A*: hsFn ×160,000 magnification, showing electron-dense cores of 7–8 nm in diameter. *B*: representative image of a cell incubated for 20 min at 37°C with 20 nM hsFn. The panel on the *right* shows a magnification of an electron-dense aggregate. *C*: image of a cell without preincubation with hsFn. Note the absence of large electron-dense cores.

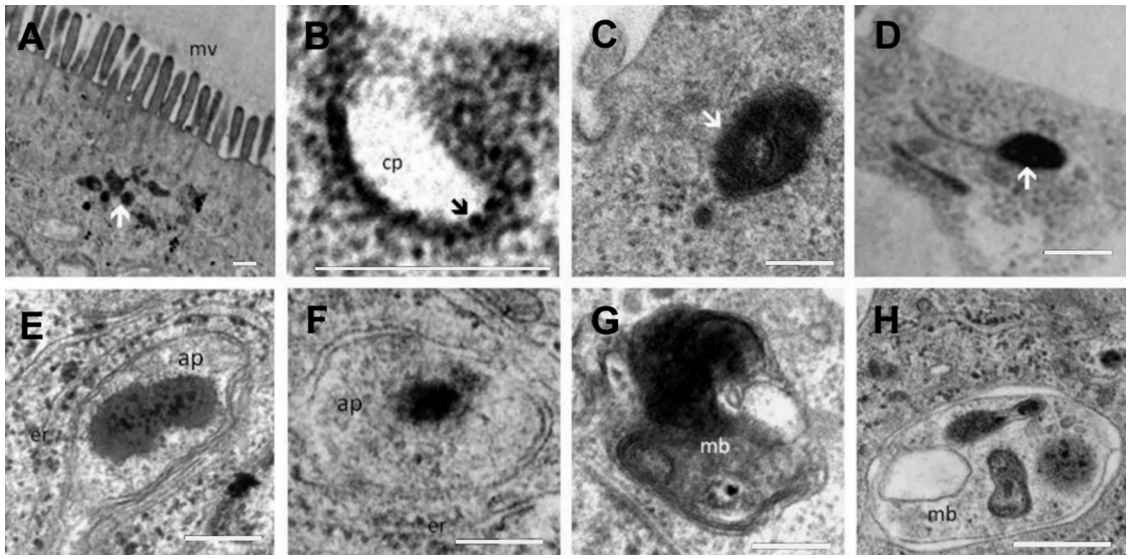

Fig. 4. Distribution of internalized hsFn detected by transmission electron microscopy. Caco-2 cells grown in bicameral inserts were incubated for 45 min with 20 nM hsFn in DMEM before processing for transmission electron microscopy. *A*: view of the apical region of the cells showing microvilli (mv) and electron-dense material in intracellular structures (arrow). *B*: plasma membrane-coated pit (cp) containing hsFn (arrow). *C* and *D*: tubular-vesicular structures in the peripheral cytoplasm containing hsFn (arrows). *E* and *F*: double-membrane structures, containing hsFn and amorphous electron-dense material, interpreted as autophagosomes (ap). These structures were seen invariantly surrounded by rough endoplasmic reticulum (er). *G* and *H*: multivesicular bodies (mb) containing hsFn and amorphous electron-dense material. Scale bars are 200 nm.

gosomes (33, 47, 56) (Fig. 4, *E* and *F*). These structures enclosed hemosiderin bodies consistent with individual hsFn molecules aggregating into electron-dense bodies. These hemosiderin bodies have been described as the initial product of ferritin degradation in iron-loaded cells (15, 42). In addition, we detected hsFn in electron-dense multimembranous bodies reminiscent of multivesicular bodies and autolysosomes (Fig. 4, *G* and *H*).

Inhibition of lysosome or autophagosome activity decreases the degradation of hsFn. The generation of trichloroacetic acid (TCA)-soluble radioactivity from radioactive-labeled proteins is an established criterion to evaluate autophagic or lysosomal activity (10). To evaluate further the role of autophagosomes and lysosomes in hsFn degradation, we analyzed the TCA-soluble material from cells incubated with ^{131}I-labeled hsFn under conditions of inhibition of lysosomal (chloroquine) or autophagosomal (3-MA) activity (Fig. 5). Both chloroquine and 3-MA treatments significantly inhibited hsFn degradation ($P < 0.001$ compared with control cells). As expected, degradation was largely inhibited (to 14.8% of control) in cells incubated a 4°C, an indication that degradation requires an active endocytic process. It is important to note that the inhibitors 3-ME and chloroquine are not specific for the autophagosomic or the endocytic processes; thus, off-target effects cannot be ruled out.

The sum of the above evidence suggests that, at the onset of the endocytic process, exogenous hsFn is internalized via clathrin-coated pits. After internalization, hsFn follows a degradation pathway that includes early endosomes, autophagosomes, and autolysosomes.

DISCUSSION

Endocytosis of the ferritin molecule is a highly efficient mechanism for the absorption of hundreds or thousands of dietary iron atoms per endocytic event (54). Knowledge on the cellular and molecular structures associated with this process becomes relevant to understand this new route of body iron acquisition. In the present study, we identified in Caco-2 cells, a model of intestinal epithelia, the endosomal compartments that exogenous hsFn reaches before its intracellular degradation. We found both by confocal and transmission electron microscopy that hsFn internalizes via clathrin-coated pits. Because clathrin-mediated endocytosis involves the recruitment of specific receptors into coated pits, our findings lend

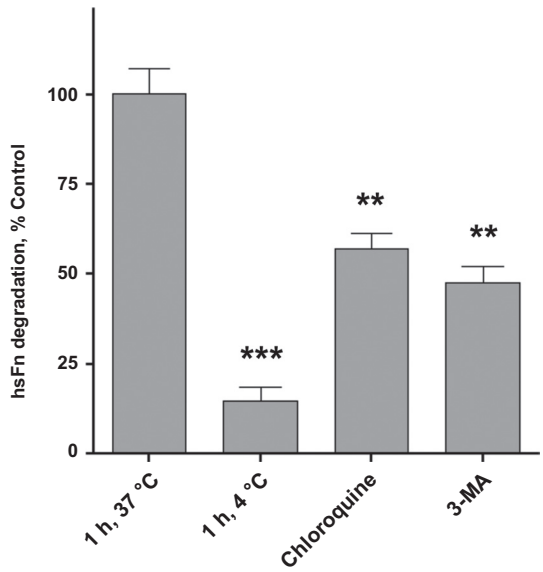

Fig. 5. Effect of lysosomal and autophagosomal inhibitors on ^{131}I-labeled hsFn degradation. Cells were incubated for 60 min at 37°C with 20 nM ^{125}I-labeled hsFn in the absence (control) or the presence of 10 mM 3-MA or 100 μM chloroquine. As a negative control, cells were incubated with ^{125}I-labeled hsFn for 1 h at 4°C. Values represent means ± SE of a representative experiment ($n = 3$). $^{**}P < 0.01$ and $^{***}P < 0.001$ by Dunnett's post hoc test.

support to the presence of specific ferritin receptors on the apical surface of absorptive enterocytes, such as polymeric immunoglobulin and low-density lipoprotein receptors (3, 16).

The question arises as to the nature of the ferritin receptor in enterocytes since, as mentioned before, three proteins have been identified in this class: TIM-2, Scara5, and TfR1. TIM-2 is strongly regulated by cell iron levels, but it does not seem to be a likely enterocyte ferritin candidate since its expression is restricted to immune system cells (5, 44). The bacteria-scavenger receptor Scara5 is another possible candidate for an enterocyte ferritin receptor. Scara5 expression is mostly associated to epithelia cells, although, at difference with TIM-2, cell iron levels do not regulate its expression (17). In addition, the presence of Scara5 in intestinal epithelia cells has not been reported. TfR1 is yet another possible candidate; it is expressed in enterocytes where it mediates basolateral iron uptake (37), and the enterocyte apical membrane contains TfR1 (21). Hence, TfR1 is present in the right cell type and in the correct cellular localization.

In this work, we found that internalized hsFn codistributed with the early endosome marker EEA1. Similarly, by transmission electron microscopy, we detected hsFn in tubulevesicular structures near the apical plasma membrane. These observations indicate that, after internalization, hsFn was delivered to early endosomes. In canonical receptor-mediated endocytosis, early endosomes mature into late endosomes, multivesicular bodies, and lysosomes (27). Most probably internalized hsFn partly followed this path since it codistributed with the lysosomal marker LAMP2, and its degradation was inhibited by the lysosomotropic agent chloroquine.

Electron microscopy of cells incubated with hsFn revealed purported ferritin granules in double-membrane compartments with the morphological features of autophagosomes. The discovery of hsFn in these compartments prompted us to evaluate its possible passage through autophagic compartments. Cells widely use the autophagosome-autolysosome route for degradation of senescent organelles and protein aggregates (9, 29, 31). Within this route, fusion of autophagosomes with lysosomes bring about the process by which autophagosomal content reaches lysosomes. Our confocal microscopy experiments indicated the codistribution of hsFn with LC3-positive compartments. Moreover, serum starvation, which stimulates autophagy, resulted in increased intracellular hsFn, whereas inhibition of autophagy with 3-ME resulted in decreased intracellular hsFn. These observations indicate that, in its degradation route, exogenous hsFn traffics through autophagic compartments before its destination to lysosomes. The signal of hsFn fluorescence codistributing with the lysosome marker LAMP2 was smaller than that codistributing with the autophagosome marker LC3 (compare Figs. 1*C* and 2*A*), suggesting that the hsFn protein coat was degraded upon reaching lysosomes.

The question remains as to whether ferritin endocytosis responds to the requirements of iron of the enterocyte or responds to a mechanism aimed to provide amino acids under starvation conditions. In preliminary experiments, we found that endocytosis of hsFn had a similar rate in iron-replete and in iron-starving cells (data not shown), whereas stimulation of autophagy by serum depletion increased the amount of internalized hsFn and the degree of codistribution between LC3 and hsFn (Fig. 2*B*). These observations suggest that ferritin endocytosis responds to starvation rather than to iron deficiency signals, although further experiments are needed to analyze specifically this point.

In summary, our previous results (45, 54) and those of this study are consistent with a mechanism for dietary iron absorption in which iron-loaded ferritin binds to a receptor in the apical membrane of the enterocyte and is internalized via clathrin-coated pits. Once inside the cell, ferritin follows a degradation route through early endosomes, autophagosomes, and lysosomes, which digest the protein coat and deliver the ferritin-associated iron to the cytoplasm by a slow-release mechanism. Two future questions arising from this study entail *1*) the nature of the intestinal ferritin receptor and, most important, *2*) the signals that govern ferritin endocytosis by the enterocyte.

GRANTS

This work was financed by project ICM-P05-001-F from the Millennium Scientific Initiative, Ministerio de Economía, Chile (to M. T. Núñez), and by Grants 1070840 from Fondo Nacional de Ciencia y Tecnología (to M. T. Núñez) and ACT 1111 (to S. Lavandero and M. Chiong).

DISCLOSURES

No conflicts of interest, financial or otherwise, are declared by the authors.

AUTHOR CONTRIBUTIONS

Author contributions: E.A., C.G., V.T., J.P.M., M.C., F.N., and J.F. performed experiments; E.A., C.G., V.T., J.P.M., S.L., J.F., and M.T.N. analyzed data; E.A., J.F., and M.T.N. interpreted results of experiments; E.A., J.P.M., S.L., J.F., and M.T.N. edited and revised manuscript; J.F. and M.T.N. prepared figures; M.T.N. conception and design of research; M.T.N. drafted manuscript; M.T.N. approved final version of manuscript.

REFERENCES

1. **Adams PC, Powell LW, Halliday JW.** Isolation of a human hepatic ferritin receptor. *Hepatology* 8: 719–721, 1988.
2. **Ainsworth SK, Karnovsky MJ.** An ultrastructural staining method for enhancing the size and electron opacity of ferritin in thin sections. *J Histochem Cytochem* 20: 225–229, 1972.
3. **Asano M, Komiyama K.** Polymeric immunoglobulin receptor. *J Oral Sci* 53: 147–156, 2011.
4. **Blommaart EF, Krause U, Schellens JP, Vreeling-Sindelarova H, Meijer AJ.** The phosphatidylinositol 3-kinase inhibitors wortmannin and LY294002 inhibit autophagy in isolated rat hepatocytes. *Eur J Biochem* 243: 240–246, 1997.
5. **Chen TT, Li L, Chung DH, Allen CD, Torti SV, Torti FM, Cyster JG, Chen CY, Brodsky FM, Niemi EC, Nakamura MC, Seaman WE, Daws MR.** TIM-2 is expressed on B cells and in liver and kidney and is a receptor for H-ferritin endocytosis. *J Exp Med* 202: 955–965, 2005.
6. **Fernandez J, Valladares M, Fuentes R, Ubilla A.** Reorganization of cytoplasm in the zebrafish oocyte and egg during early steps of ooplasmic segregation. *Dev Dyn* 235: 656–671, 2006.
7. **Fisher J, Devraj K, Ingram J, Slagle-Webb B, Madhankumar AB, Liu X, Klinger M, Simpson IA, Connor JR.** Ferritin: a novel mechanism for delivery of iron to the brain and other organs. *Am J Physiol Cell Physiol* 293: C641–C649, 2007.
8. **Florey O, Overholtzer M.** Autophagy proteins in macroendocytic engulfment. *Trends Cell Biol* 22: 374–380, 2012.
9. **Glick D, Barth S, Macleod KF.** Autophagy: cellular and molecular mechanisms. *J Pathol* 221: 3–12, 2010.
10. **Goldstein JL, Brown MS.** Binding and degradation of low density lipoproteins by cultured human fibroblasts. Comparison of cells from a normal subject and from a patient with homozygous familial hypercholesterolemia. *J Biol Chem* 249: 5153–5162, 1974.
11. **Han J, Seaman WE, Di X, Wang W, Willingham M, Torti FM, Torti SV.** Iron uptake mediated by binding of H-ferritin to the TIM-2 receptor in mouse cells. *PLoS One* 6: e23800, 2011.

12. **Harrison PM, Arosio P.** The ferritins: molecular properties, iron storage function and cellular regulation. *Biochim Biophys Acta* 1275: 161–203, 1996.
13. **Hultcrantz R, Glaumann H.** Intracellular fate of ferritin in HeLa cells following microinjection. *Exp Cell Res* 171: 203–212, 1987.
14. **Hurrell R, Egli I.** Iron bioavailability and dietary reference values. *Am J Clin Nutr* 91: 1461S–1467S, 2010.
15. **Iancu TC.** Ultrastructural aspects of iron storage, transport and metabolism. *J Neural Transm* 118: 329–335, 2011.
16. **Jia L, Betters JL, Yu L.** Niemann-pick C1-like 1 (NPC1L1) protein in intestinal and hepatic cholesterol transport. *Annu Rev Physiol* 73: 239–259, 2011.
17. **Jiang Y, Oliver P, Davies KE, Platt N.** Identification and characterization of murine SCARA5, a novel class A scavenger receptor that is expressed by populations of epithelial cells. *J Biol Chem* 281: 11834–11845, 2006.
18. **Kalgaonkar S, Lonnerdal B.** Receptor-mediated uptake of ferritin-bound iron by human intestinal Caco-2 cells. *J Nutr Biochem* 20: 304–311, 2009.
19. **Karnovsky M.** A formaldehyde-glutaraldehyde fixative of high osmomolarity for use in electron microscopy (Abstract). *J Cell Biol* 27: 137A, 1965.
20. **Knight A, Hughson E, Hopkins CR, Cutler DF.** Membrane protein trafficking through the common apical endosome compartment of polarized Caco-2 cells. *Mol Biol Cell* 6: 597–610, 1995.
21. **Kolachala VL, Sesikeran B, Nair KM.** Evidence for a sequential transfer of iron amongst ferritin, transferrin and transferrin receptor during duodenal absorption of iron in rat and human. *World J Gastroenterol* 13: 1042–1052, 2007.
22. **Laftah AH, Latunde-Dada GO, Fakih S, Hider RC, Simpson RJ, McKie AT.** Haem and folate transport by proton-coupled folate transporter/haem carrier protein 1 (SLC46A1). *Br J Nutr* 101: 1150–1156, 2009.
23. **Le Brun NE, Crow A, Murphy ME, Mauk AG, Moore GR.** Iron core mineralisation in prokaryotic ferritins. *Biochim Biophys Acta* 1800: 732–744, 2010.
24. **Li JY, Paragas N, Ned RM, Qiu A, Viltard M, Leete T, Drexler IR, Chen X, Sanna-Cherchi S, Mohammed F, Williams D, Lin CS, Schmidt-Ott KM, Andrews NC, Barasch J.** Scara5 is a ferritin receptor mediating non-transferrin iron delivery. *Dev Cell* 16: 35–46, 2009.
25. **Li L, Fang CJ, Ryan JC, Niemi EC, Lebron JA, Bjorkman PJ, Arase H, Torti FM, Torti SV, Nakamura MC, Seaman WE.** Binding and uptake of H-ferritin are mediated by human transferrin receptor-1. *Proc Natl Acad Sci USA* 107: 3505–3510, 2010.
26. **Lonnerdal B, Bryant A, Liu X, Theil EC.** Iron absorption from soybean ferritin in nonanemic women. *Am J Clin Nutr* 83: 103–107, 2006.
27. **Luzio JP, Parkinson MD, Gray SR, Bright NA.** The delivery of endocytosed cargo to lysosomes. *Biochem Soc Trans* 37: 1019–1021, 2009.
28. **Macara IG, Hoy TG, Harrison PM.** The formation of ferritin from apoferritin. Inhibition and metal ion-binding studies. *Biochem J* 135: 785–789, 1973.
29. **Majeski AE, Dice JF.** Mechanisms of chaperone-mediated autophagy. *Int J Biochem Cell Biol* 36: 2435–2444, 2004.
30. **Mann S, Williams JM, Treffry A, Harrison PM.** Reconstituted and native iron-cores of bacterioferritin and ferritin. *J Mol Biol* 198: 405–416, 1987.
31. **Massey A, Kiffin R, Cuervo AM.** Pathophysiology of chaperone-mediated autophagy. *Int J Biochem Cell Biol* 36: 2420–2434, 2004.
32. **Mehrpour M, Esclatine A, Beau I, Codogno P.** Autophagy in health and disease. I. Regulation and significance of autophagy: an overview. *Am J Physiol Cell Physiol* 298: C776–C785, 2010.
33. **Mizushima N.** Methods for monitoring autophagy. *Int J Biochem Cell Biol* 36: 2491–2502, 2004.
34. **Mortimore GE, Poso AR.** Intracellular protein catabolism and its control during nutrient deprivation and supply. *Annu Rev Nutr* 7: 539–564, 1987.
35. **Moss D, Fargion S, Fracanzani AL, Levi S, Cappellini MD, Arosio P, Powell LW, Halliday JW.** Functional roles of the ferritin receptors of human liver, hepatoma, lymphoid and erythroid cells. *J Inorg Biochem* 47: 219–227, 1992.
36. **Núñez MT.** Regulatory mechanisms of intestinal iron absorption-uncovering of a fast-response mechanism based on DMT1 and ferroportin endocytosis. *Biofactors* 36: 88–97, 2010.
37. **Núñez MT, Tapia V, Arredondo M.** Intestinal epithelia (Caco-2) cells acquire iron through the basolateral endocytosis of transferrin. *J Nutr* 126: 2151–2158, 1996.
38. **Petiot A, Ogier-Denis E, Blommaart EF, Meijer AJ, Codogno P.** Distinct classes of phosphatidylinositol 3′-kinases are involved in signaling pathways that control macroautophagy in HT-29 cells. *J Biol Chem* 275: 992–998, 2000.
39. **Ponka P, Beaumont C, Richardson DR.** Function and regulation of transferrin and ferritin. *Semin Hematol* 35: 35–54, 1998.
40. **Qiu A, Jansen M, Sakaris A, Min SH, Chattopadhyay S, Tsai E, Sandoval C, Zhao R, Akabas MH, Goldman ID.** Identification of an intestinal folate transporter and the molecular basis for hereditary folate malabsorption. *Cell* 127: 917–928, 2006.
41. **Ramm GA, Britton RS, O'Neill R, Bacon BR.** Identification and characterization of a receptor for tissue ferritin on activated rat lipocytes. *J Clin Invest* 94: 9–15, 1994.
42. **Richter GW.** A study of hemosiderosis with the aid of electron microscopy; with observations on the relationship between hemosiderin and ferritin. *J Exp Med* 106: 203–218, 1957.
43. **Rodriguez-Boulan E, Kreitzer G, Musch A.** Organization of vesicular trafficking in epithelia. *Nat Rev Mol Cell Biol* 6: 233–247, 2005.
44. **Rodriguez-Manzanet R, DeKruyff R, Kuchroo VK, Umetsu DT.** The costimulatory role of TIM molecules. *Immunol Rev* 229: 259–270, 2009.
45. **San Martin CD, Garri C, Pizarro F, Walter T, Theil EC, Núñez MT.** Caco-2 intestinal epithelial cells absorb soybean ferritin by mu2 (AP2)-dependent endocytosis. *J Nutr* 138: 659–666, 2008.
46. **Shayeghi M, Latunde-Dada GO, Oakhill JS, Laftah AH, Takeuchi K, Halliday N, Khan Y, Warley A, McCann FE, Hider RC, Frazer DM, Anderson GJ, Vulpe CD, Simpson RJ, McKie AT.** Identification of an intestinal heme transporter. *Cell* 122: 789–801, 2005.
47. **Stromhaug PE, Berg TO, Fengsrud M, Seglen PO.** Purification and characterization of autophagosomes from rat hepatocytes. *Biochem J* 335: 217–224, 1998.
48. **Takami M, Mizumoto K, Kasuya I, Kino K, Sussman HH, Tsunoo H.** Human placental ferritin receptor. *Biochim Biophys Acta* 884: 31–38, 1986.
49. **Takatsuka C, Inoue Y, Matsuoka K, Moriyasu Y.** 3-methyladenine inhibits autophagy in tobacco culture cells under sucrose starvation conditions. *Plant Cell Physiol* 45: 265–274, 2004.
50. **Tanida I, Ueno T, Kominami E.** LC3 conjugation system in mammalian autophagy. *Int J Biochem Cell Biol* 36: 2503–2518, 2004.
51. **Tapia V, Arredondo M, Núñez MT.** Regulation of Fe absorption by cultured intestinal epithelia (Caco-2) cell monolayers with varied Fe status. *Am J Physiol Gastrointest Liver Physiol* 271: G443–G447, 1996.
52. **Theil EC.** Ferritin protein nanocages use ion channels, catalytic sites, and nucleation channels to manage iron/oxygen chemistry. *Curr Opin Chem Biol* 15: 304–311, 2011.
53. **Theil EC.** Iron, ferritin, nutrition. *Annu Rev Nutr* 24: 327–343, 2004.
54. **Theil EC, Chen H, Miranda C, Janser H, Elsenhans B, Núñez MT, Pizarro F, Schumann K.** Absorption of iron from ferritin is independent of heme iron and ferrous salts in women and rat intestinal segments. *J Nutr* 142: 478–483, 2012.
55. **Todorich B, Zhang X, Slagle-Webb B, Seaman WE, Connor JR.** Tim-2 is the receptor for H-ferritin on oligodendrocytes. *J Neurochem* 107: 1495–1505, 2008.
56. **Vincent RA Jr, Spicer SS.** Giant dense bodies in fibroblasts cultured from beige mice with the Chediak-Higashi syndrome. *Am J Pathol* 105: 270–278, 1981.
57. **Wibo M, Poole B.** Protein degradation in cultured cells. II. The uptake of chloroquine by rat fibroblasts and the inhibition of cellular protein degradation and cathepsin B1. *J Cell Biol* 63: 430–440, 1974.